Pion scattering from polarized ^{15}N at $T_\pi = 164$ MeV

R. Meier, E. T. Boschitz, S. Ritt, R. Tacik,* and M. Wessler
Kernforschungszentrum Karlsruhe, Institut für Kernphysik und Institut für Experimentelle Kernphysik der Universität Karlsruhe, 7500 Karlsruhe, Federal Republic of Germany

J. A. Konter, S. Mango, D. Renker, and B. van den Brandt
Paul Scherrer Institute, 5232 Villigen, Switzerland

W. Meyer and W. Thiel
Physikalisches Institut, University of Bonn, 5300 Bonn, Federal Republic of Germany

R. Mach
Institute of Nuclear Physics, Československá Akademie Věd, 25068 Řež, Czechoslovakia

P. Amaudruz, R. R. Johnson, G. R. Smith, and P. Weber
TRIUMF and University of British Columbia, Vancouver, British Columbia, Canada
(Received 13 February 1990)

The analyzing power A_y was measured for $\pi^+ - {}^{15}\vec{\mathrm{N}}$ elastic scattering at $T_\pi = 164$ MeV between 40° and 100° using a polarized $^{15}NH_3$ target. Within the statistical accuracy of the data $A_y(\theta)$ was found to be zero over the full angular range. These data together with differential cross sections from the literature are compared with theoretical predictions based on a momentum-space coupled-channel formalism. While the cross section is very well reproduced there are large discrepancies in the analyzing power for which large spin effects are predicted close to the cross-section minima. Possible deficiencies in the theoretical model are discussed.

I. INTRODUCTION

Since the advent of the pion factories, a vast amount of precise pion scattering data has been accumulated, particularly in the region of the $\Delta(3,3)$ resonance.[1] The theoretical models used to describe these data were based either on multiple-scattering expansions[2-6] or the concept of the isobar-doorway model.[7-10] A truly microscopic description was not achieved in either case since, in one way or another, the pion interaction with two or more nucleons had to be treated on a phenomenological level. In the case of the multiple-scattering models the optical potential was supplemented by a second-order term proportional to the square of the nuclear density, while in the isobar-doorway model a spreading potential was introduced. All of these models have been quite successful in reproducing elastic cross sections over the forward hemisphere; however, there were problems at larger angles, even after including the second-order terms. From this, one might conclude that some reaction dynamics in π-nuclear scattering are still missing in these calculations.

In π-nuclear scattering so far only cross-section data have been accumulated. These data are sensitive mainly to the spin-independent part of the interaction. The only data which involve magnetic substates for the target nucleus came from π-γ angular correlation measurements in the $^{12}C(\pi,\pi'\gamma)$ reaction.[11] The γ decay of the aligned 2^+ state (4.44 MeV) was measured in coincidence with the scattered pions. These data provided a sensitive test of nuclear models. The data at a momentum transfer less than that at the first maximum in the differential cross section gave clear preference to the Δ-hole model over the standard (static) pion-nucleus scattering model. This demonstrates that observables which involve the spin state of the target nucleus could provide new information. Such observables may be the vector or tensor analyzing power in pion-scattering from polarized complex nuclei. The vector analyzing power, for example, depends on the product of the non-spin-flip and spin-flip parts of the reaction amplitude, and not on the sum of the squares of both amplitudes, as for cross sections. Therefore, interferences between these amplitudes may sufficiently enhance spin effects which are otherwise not detectable.

Due to the lack of data on the spin dependence in pion-nuclear scattering there has been little theoretical interest in the past. Now, with the increasing availability of polarized nuclear targets, and consequently the prospect of novel experiments, this attitude is changing. A recent workshop[12] triggered a number of experimental proposals, and the number of theoretical calculations is steadily increasing. So far, predictions for the polarization observables A_y or iT_{11} exist for the nuclei ^{3}He (Refs. 13-17), ^{6}Li (Refs. 18-20), ^{13}C (Refs. 15 and 21), ^{14}N and ^{15}N (Ref. 22). When comparing the predictions of the different theoretical models one finds large differences, but also common features. For nuclei with $A = 13$ to 15, the analyzing power seems to reflect the diffraction pattern of the cross-section angular distributions. The larg-

est analyzing power is predicted close to the minima of the differential cross section where the dominant non-spin-flip scattering is small. One should note, however, that in this particular region theoretical predictions may be unreliable due to delicate interferences between the non-spin-flip and spin-flip amplitude.

Measurements of the analyzing power A_y in π^+-$^{15}\vec{\text{N}}$ scattering[23] at $T_\pi = 164$ MeV in the angular range between 40° and 100° c.m. are reported in detail in this work. The target, energy, and angular range were chosen for both experimental and theoretical reasons. The experimental reasons include the availability of a suitable chemical compound for ^{15}N, namely, $^{15}NH_3$; the kinematical separation between H and N; and the energy separation between the ground and excited states in ^{15}N, which is sufficient for the overall energy resolution of our pion scattering facility (including the polarized target) which is typically 1.5–2 MeV. In addition, adequate nuclear polarization, which can be measured with a standard NMR technique could be obtained for ^{15}N.

The theoretical reasons include the fact that the nucleus ^{15}N is a typical shell-model nucleus with a reasonably well-known wave function. In the single-particle model the ground-state magnetic moment of a $1p_{1/2}$ hole is $\mu = -0.263\mu_n$, to be compared with the experimental value for ^{15}N, $\mu = -0.283\mu_n$. Theoretical predictions by Mach and Kamalov[22] indicate a large analyzing power at 164 MeV in the angular range chosen.

II. THE EXPERIMENT

A. Method

For a spin-$\frac{1}{2}$ nucleus, such as ^{15}N, the analyzing power A_y (more correctly A_{0y} since the target and not the projectile is polarized) is calculated from the measured cross sections σ^+ and σ^-, where the "+" and "−" indicate the corresponding target polarizations p^+ and p^-, according to

$$A_y = \frac{\sigma^+ - \sigma^-}{\sigma^+ p^- + \sigma^- p^+} , \tag{1}$$

where the subscript + (−) for p indicates the direction parallel (antiparallel) to the quantization axis of the polarized target, defined as $\mathbf{n} = \mathbf{k} \times \mathbf{k}'$ ($\mathbf{k}$ being the momentum of the incident, $\mathbf{k}'$ of the scattered pion). The target polarization p is defined as $p = n^+ - n^-$ ($p^\pm$ for $n^+ \gtrless n^-$) with $n^+ + n^- = 1$, where n^+ and n^- stand for the population of the ^{15}N magnetic substates $m = +\frac{1}{2}$ and $m = -\frac{1}{2}$, respectively. The uncertainty in A_y is obtained from

$$\Delta A_y = \frac{\{(p^+ + p^-)^2[(\sigma^- \Delta\sigma^+)^2 + (\sigma^+ \Delta\sigma^-)^2] + (\sigma^+ - \sigma^-)^2[(\sigma^- \Delta p^+)^2 + (\sigma^+ \Delta p^-)^2]\}^{1/2}}{(p^- \sigma^+ + p^+ \sigma^-)^2} . \tag{2a}$$

In the case of $\sigma^+ \sim \sigma^- = \sigma$ and $p^+ \sim p^- = p$ this expression reduces to

$$\Delta A_y = \frac{1}{2p} \left[\left(\frac{\Delta\sigma^+}{\sigma} \right)^2 + \left(\frac{\Delta\sigma^-}{\sigma} \right)^2 \right]^{1/2} \tag{2b}$$

from which is is clear that a large target polarization p and/or very small uncertainties in the measured cross sections are required to obtain a small uncertainty ΔA_y.

In the past, nuclei have been polarized in two ways. One way is the "brute force" nuclear polarization where the nuclei are kept at very low temperature (few mK) in very strong magnetic fields (6–8 T) to unbalance the population of the magnetic substates at Boltzmann equilibrium. The strong magnetic fields may be produced externally or in special cases internally (crystalline fields in molecules). The brute force method may be applied to a large variety of nuclei, though it is useful only for experiments involving neutrons because the energy loss of charged particles in the sample produces too much target heating.

The other method, applied extensively to protons and deuterons, is the "dynamic" nuclear polarization by microwave irradiation. This method utilizes the fact that part of the large electron polarization obtained in paramagnetic centers for $T \leq 0.5$ K and $B \geq 2.5$ T can be transferred to the nuclear spin system by irradiating the sample with microwaves at a frequency of about 70 GHz, inducing the desired electron-nuclear spin flips. An important requirement of this method is that the electron-spin-lattice relaxation time is short, while the nuclear relaxation time is long. The state of nuclear polarization p^+ or p^- is reversed by a small change in the microwave frequency. This method also depends critically on the solid-state structure of the chemical compound, the way in which the right amount of paramagnetic centers are produced, the characteristics of the electron-spin resonance curve, the speed of polarization transfer from the electron to the nuclear spin reservoir, the homogeneity of the magnetic field and the temperature at the location of the nucleus to be polarized, etc. For this reason, after years of intensive research in several laboratories only a small variety of polarized light target nuclei, i.e., ^{6}Li, ^{7}Li, ^{13}C, ^{14}N, ^{15}N, and ^{19}F (the first two only most recently) have become available. Typical target polarizations for those nuclei are $p = 0.50$ for ^{6}Li and ^{7}Li, 0.30 for ^{13}C, 0.15 for ^{14}N and ^{15}N, and 0.70 for ^{19}F.

In addition to the problem of availability of suitable nuclei, there is the problem of energy resolution in pion scattering from a complex polarized target system. Due to the energy straggling in the target, the target walls and the helium-cooling liquid the overall energy resolution is limited typically to 1 MeV. A further severe difficulty is the large background in the pion spectra produced by

pions scattered from target walls, helium, NMR coil and last but not least from nuclei in the chemical compound other than the target nucleus. This background must be measured very carefully in separate experiments. For this reason, the unfolding of the complicated spectra produces an important contribution to the overall error in the cross sections σ^+ and σ^-. When this experiment began only the polarized nuclei ^{13}C, ^{14}N, and ^{15}N were available. Mainly for background reasons $^{15}NH_3$ was chosen for the initial experiment, in spite of the smaller target polarization in comparison to ^{13}C.

B. Experimental setup

The experiment was performed using the πM1 beam line and the SUSI pion spectrometer[24] at the Paul Scherrer Institute (formerly SIN) in Switzerland. The πM1 facility is particularly suitable for this type of experiment since it combines sufficient energy resolution for pion scattering from complex polarized nuclei with a small beam spot on a target required for the typical size of a polarized target (a few cm^3). The description of the experimental setup for polarization measurements can be found in earlier publications.[25] Here only those details important for this experiment are described.

The PSI polarized target cryostat was the same as that used for recent measurements of tensor observables in the $\pi d \rightarrow \pi d$ reaction.[26] It consists of a top-loading $^3He/^4He$ dilution refrigerator with a cooling power of about 4 mW at a temperature of 0.3 mK, and a base temperature ≤ 0.05 K. A special feature of this cryostat is the thin target cell ($5\times18\times18$ mm^3), surrounded by two more cells ($6\times19\times19$ mm^3) and ($7\times20\times20$ mm^3) which contain thin layers of the liquid $^3He/^4He$ coolant, and separate the dilution refrigerator from the isolation vacuum of the scattering chamber. The wall thickness of each cell is 0.1 mm. This compact target geometry was extremely important for the present experiment since it kept the large background from π scattering from helium within tolerable limits. At this point one should emphasize that the use of a dilution refrigerator is not only necessary for obtaining a sizable ^{15}N polarization but also important for background reasons. By suitable adjustments of the dilution refrigerator the target material is floating in the superfluid ^4He-rich phase (the phase transition being at the top of the target cell) and is evenly cooled, independent of the microwave power. Therefore the density of the liquid coolant does not change. In contrast to this, in a ^3He evaporation cryostat the density of the boiling ^3He liquid varies with the microwave power (usually different for positive and negative target polarizations) and therefore produces an ill-defined ^3He background.

The $^{15}NH_3$ target material was prepared by the polarized target group at the University of Bonn. It consisted of beads approximately 1 mm in size. The special process of preparing these samples is described in Ref. 27. The target material was polarized by irradiation with microwaves in a magnetic field of 2.5 T. The maximum positive (negative) polarization for ^{15}N which was obtained with microwave frequency 70.320 (70.670) GHz, respectively, led to $p_{max}=0.17$. Typical polarizing times (for reaching 90% of the maximum value) were 12 h. Details of the determination of the target polarization will be given in Sec. III B. Because of the relatively long polarizing times the data-taking procedure was different from that adopted in our earlier experiments.[25] Instead of reversing the polarity of the target several times while holding the spectrometer angle fixed, the entire angular distribution was measured for each sign of the target polarization before the target polarity was reversed. Three σ^+ and σ^- cycles were measured to eliminate systematic errors. This procedure of data taking, however, required a good reproducibility of the spectrometer angle setting. This was achieved to within 0.01°, as compared with the angular acceptance of the SUSI spectrometer of $\Delta\theta=9°$ resulting in an error of A_y of less than 1‰. The polarized target was carefully centered within 1 mm with respect to the axis of rotation of the spectrometer. The target angle (57.5° between the target normal and the beam direction) was kept fixed during the entire measurement to avoid systematic errors.

III. DATA REDUCTION

A. Determination of cross sections

According to Eq. (1) the analyzing power $A_y(\theta)$ is calculated from the measured cross sections $\sigma^+(\theta)$ and $\sigma^-(\theta)$ (described in this section) and the target polarizations p^+ and p^- (described in the following section). The differential cross section for π-scattering into the SUSI spectrometer is determined from the expression

$$\frac{d\sigma}{d\Omega}=\frac{Y}{n_b\epsilon_{cham}\epsilon_{comp}}\frac{1}{n_t\Delta\Omega\eta}\ , \tag{3}$$

where Y represents the number of scattering events determined from the energy loss spectrum, n_b the corresponding number of incident pions in the beam, ϵ_{cham} the combined multiwire chamber efficiency, ϵ_{comp} the computer efficiency caused by the dead time of the data acquisition system, n_t the number of target nuclei, $\Delta\Omega$ the solid angle acceptance of the spectrometer, and η the pion decay factor.

As mentioned above a crucial part of the data taking is the measurement of the background. The background from the metal target cell and the NMR coil was measured at all angles by removing the helium and the ammonia from the target cell. The background from helium was determined at angles between 40 and 80 degrees by removing the helium only and comparing foreground and "helium-removed" background spectra. Beyond 80° the helium peak was well separated from the ammonia peaks. The background spectra were corrected for the smaller energy loss and energy straggling which the pions experienced in scattering from an empty or "helium-removed" target cell. Typical foreground- and background-subtracted spectra are shown in Fig. 1. Note that the relatively large width of the π^+p scattering peak in these spectra is due to the fact that π-^{15}N scattering kinematics was used to calculate these energy-loss spectra. The background subtracted spectra were then subjected to a

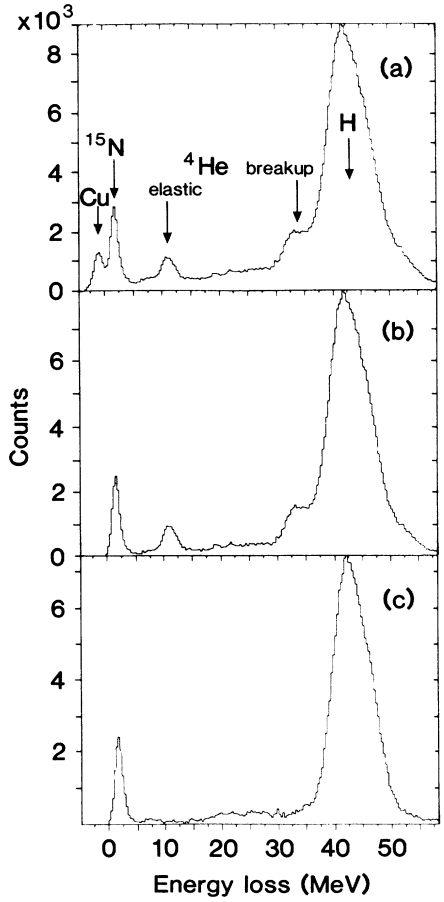

FIG. 1. Typical foreground- and background-subtracted energy-loss spectra for pion scattering from $^{15}\vec{N}H_3$ (negative target polarization). (a) full spectrum, (b) Cu background subtracted, (c) Cu+^{4}He background subtracted.

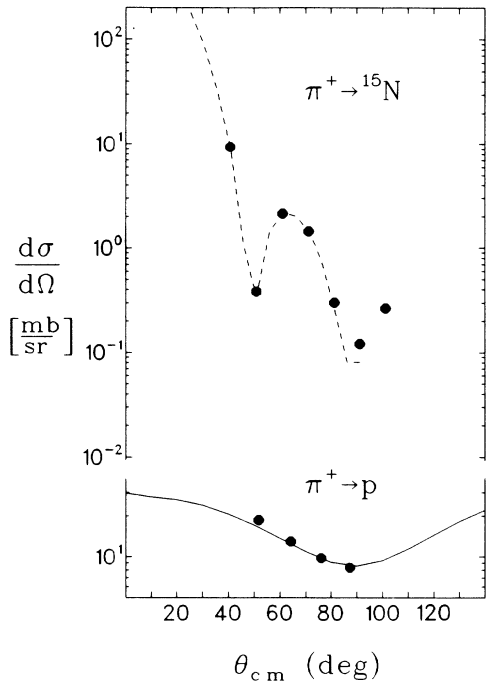

FIG. 2. Consistency test for extracting cross sections from the present polarization experiment. In the lower half of this figure relative π^+-p cross sections from this experiment (solid circles) are normalized to predictions from πN phase shifts (Ref. 28) (solid line). Applying this normalization factor "absolute" π^+-^{15}N cross sections (solid circles) are obtained and compared with data in the literature (Ref. 29), shown as dashed line.

multiple peak fitting program which incorporated information on intrinsic energy resolution of the system, scattering kinematics (including corrections for the bending of the pion trajectories in the magnetic field of the polarized target), assumptions on pion nuclear breakup reactions, etc. From these fits the yields were determined for π^+-^{15}N, π^+-^{4}He, π^+-^{3}He, and π^+-p scattering. The scattering yield from ^{3}He amounted to about 5% of ^{4}He which is consistent with the ammonia target material being entirely contained in the ^{4}He-rich phase (94%) of the ^{3}He/^{4}He dilution refrigerator. From the yields relative cross sections were obtained. The uncertainty in the cross sections was calculated from the statistical errors of the foreground and the background.

According to Eq. (1) only relative cross sections are required to calculate A_y, which means that the second factor in Eq. (3) cancels. However, for testing the consistency of our fitting procedures in extracting the yields this second factor was determined by comparing our relative πp cross sections at four angles with the predictions from the πN phase-shift program SAID.[28] A single normalization factor reproduced the angular distribution quite well (see lower part of Fig. 2). Using this normalization factor "absolute" π^+-^{15}N cross sections from this experiment (full circles in the upper part of Fig. 2) can be compared with data in literature[29] displayed as the dashed line. There is good agreement over the full angular distribution. Agreement at the level of 10–15 % was also obtained between π^+-^{4}He data from the literature[30] (interpolated at our energy) and π^+-^{4}He cross sections from this experiment, by making reasonable estimates for the amount of ^{4}He contained in the target cell.

In Fig. 3 spectra normalized to equal numbers of pions incident on the target are compared for the two polarization states. The solid line corresponds to spectra obtained with positive, the dashed line with negative polarization. As one can see from the difference, there is a large asymmetry for π^+-p scattering.

B. Determination of the target polarization

The ^{15}N polarization was determined by measuring the absorptive part of the nuclear magnetic resonance (NMR) signal detected with a constant-current Q meter. With a computer-controlled frequency synthesizer a frequency range from 10 814 400 to 10 856 500 Hz was swept through in steps of 100 Hz. The output was fed into a resonance circuit, which consisted of a pickup coil, positioned in the median plane of the target container, connected to a Ga-As variable capacitor diode (Varicap) by a section of 50-Ω coaxial cable 18 cm long. The Varicap

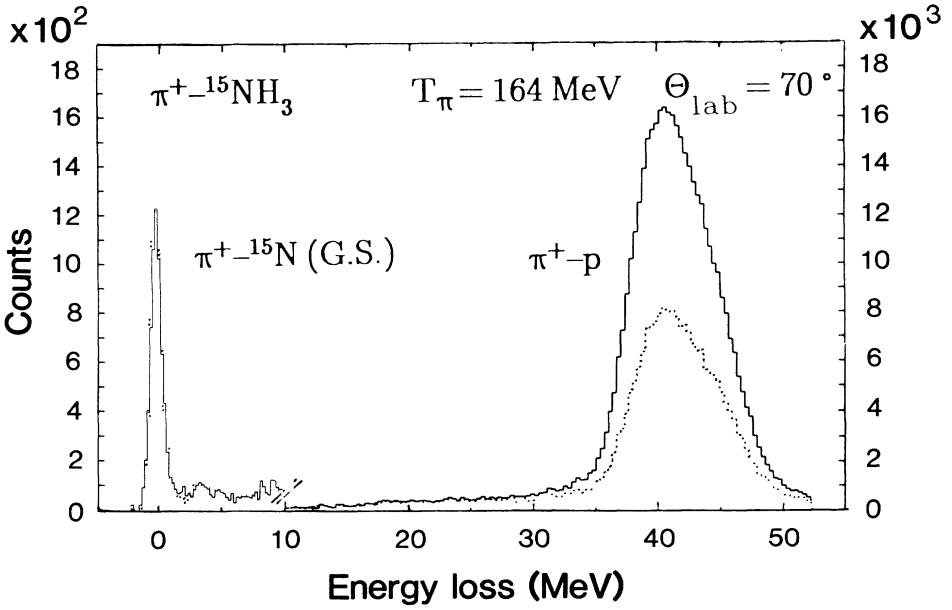

FIG. 3. Comparison of corresponding energy-loss spectra for positive (solid line) and negative (dotted line) target polarization. Note the large asymmetry in π^+-p scattering in comparison to the near zero asymmetry in π^+-$^{15}\vec{N}$ scattering.

was directly connected to the input of a field-effect transistor (FET) amplifier, both of which were capable of operating at temperatures of ~0.7 K. The characteristics for the resonance-frequency dependence of the Varicap voltage were measured and parametrized by fitting a polynomial of sixth degree. This made it possible to calculate, for each frequency set by the synthesizer, the right Varicap voltage to keep the circuit in resonance. In this way, frequency-dependent distortions of the NMR signal due to the high Q available were kept minimal. The high-frequency signal across the resonance circuit was amplified and rectified before being sent to a 12-bit analog-to-digital converter (ADC). The absolute magnitude of the vector polarization p was obtained by comparing the integral of the thermal equilibrium (TE) NMR signal with that of the dynamically enhanced polarized signal. From this ratio the target polarization was calculated. Typical thermal equilibrium (TE) and dynamical (dyn) signals are shown in Figs. 4(a) and 4(b). The TE polarization was calculated from the known temperature T and the magnetic field B according to

$$p(\mathrm{TE})=\tanh(\mu B/kT)\ ,$$

where $\mu=-0.892\times10^{-14}$ MeV/T is the ^{15}N magnetic moment, and k is the Boltzmann constant. In this experiment ($B=2.5$ T and $T=1.01$ K) a value of $p(\mathrm{TE})=2.85\times10^{-4}$ was obtained. The polarization of the dynamically polarized target can then be deduced directly from

$$p(\mathrm{dyn})=\frac{A(\mathrm{dyn})}{A(\mathrm{TE})}p(\mathrm{TE})\ ,$$

where $A(\mathrm{dyn})$ is the integral of the dynamical NMR signal and $A(\mathrm{TE})$ the corresponding integral of the thermal equilibrium NMR signal. Typical values obtained for p^+ and p^- were 0.15. The uncertainty in the determination of the TE signal (typically 5%) is mainly due to uncertainties in measuring the temperature and results in a relative normalization error in A_y of 5%. During the experiment the TE signal was measured repeatedly, and

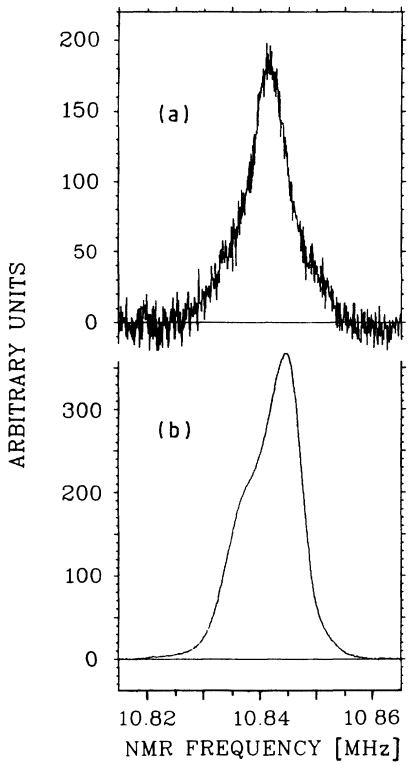

FIG. 4. Typical thermal equilibrium (TE) signal (a) and dynamically enhanced signal (b) from polarized ^{15}N nucleus.

consistent values were obtained.

The polarization of the protons in the $^{15}NH_3$ target could not be determined during the scattering experiment because the inductance of the NMR resonance circuit was tuned for the very small magnetic moment of ^{15}N. Recently, in a laboratory experiment both the ^{15}N and the H polarizations were measured simultaneously for the same target material as in the scattering experiment to establish the relationship between both polarizations. From these results the proton polarization was determined.

C. Determination of analyzing power

Three methods have been used to determine the analyzing power A_y from the measured cross sections σ^+ and σ^-. We call these the "fitting," "permutation," and "summation" methods. The "fitting" method is based on the relationship

$$\sigma^{\text{pol}}(p)=\sigma^0+\sigma^0 A_y \cdot p \tag{4}$$

where σ^0 is the cross section for zero polarization and A_y is the analyzing power. This equation has the form $y=A+B\cdot x$ so that one can fit a straight line through the σ^+ and σ^- data plotted versus the corresponding p^+ and p^- values. From the parameters A and B the values σ^0 and A_y can be determined. The uncertainty in A_y is calculated from the errors in the fitting parameters A and B. With this method a mean value for A_y is obtained, weighting the separate measurements according to their individual errors in the yields and target polarizations.

In the "permutation" method the analyzing power A_y is calculated for each possible combination pair of σ^+ and σ^-. This method gives the possibility to identify inconsistencies in the data set. Then the average of all calculated values A_y is taken. The error is determined as the mean of the errors calculated for all independent permutations.

The "summation" method consists of summing all yields of the spectra for one angle, and determining the yield for the summed spectra. The polarization corresponding to this sum is calculated as a beam-weighted average of the individual polarizations. A_y is then calculated according to Eq. (1).

The different methods produced consistent results. Therefore, the average value from the three methods was taken as the final value of A_y. The errors in A_y were found to be almost the same for the three methods; the largest was taken as the final error.

IV. RESULTS AND DISCUSSION

The analyzing power for π^+p scattering from this experiment is compared to recent measurements by Sevior *et al.*[31] and the prediction from the phase-shift analysis by Arndt and Roper.[28] Very consistent results are obtained as can be seen in Fig. 5.

The results for A_y for π^+ elastic scattering from polarized ^{15}N are listed in Table I and shown in Fig. 6 together with the cross-section data from Ref. 29. Note, that in the final data reduction the values for A_y hardly changed from the ones presented in Ref. 23, but the errors of A_y increased slightly.

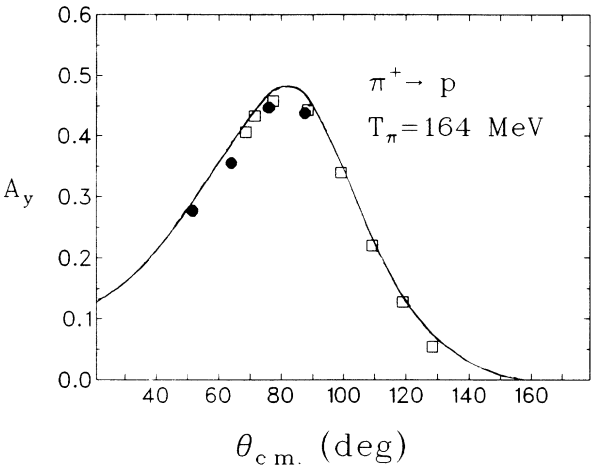

FIG. 5. The analyzing power A_y for π^+p scattering. Solid circles are from the present experiment, open squares from Ref. 31. In both cases the error bars are smaller than the size of the symbols. The solid line is the prediction from Ref. 28.

The experimental data are compared to theoretical predictions calculated with the model of Mach and Kamalov. This model was described in detail elsewhere,[22] therefore we comment here only on its basic ingredients. The pion-nucleus scattering matrix is given as

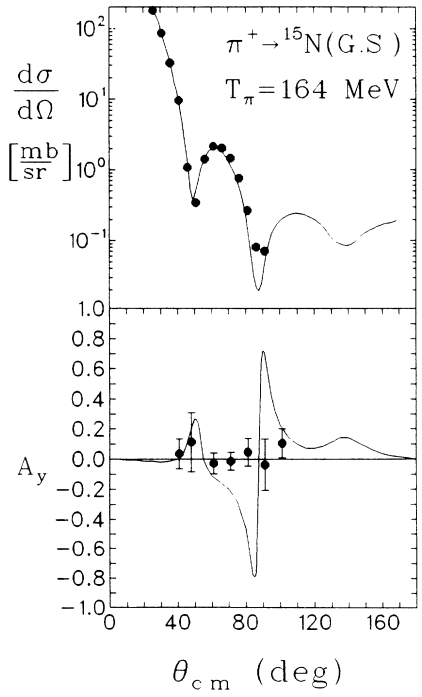

FIG. 6. The analyzing power A_y (present experiment) and $d\sigma/d\Omega$ (Ref. 29) for π^+-^{15}N scattering compared with predictions from R. Mach (Ref. 22).

TABLE I. Results for A_y from the present experiment ($T_\pi = 164$ MeV) for ^{15}N ground state.

θ_{lab} (deg)	$\theta_{c.m}$ (deg)	A_y	ΔA_y
40	40.8	+0.035	±0.099
47	48.0	+0.112	±0.198
60	61.1	−0.029	±0.069
70	71.2	−0.015	±0.058
80	81.2	+0.045	±0.091
90	91.2	−0.038	±0.170
100	101.2	+0.104	±0.096

a solution of

$$T(E)=V(E)+V(E)PG(E)T(E)\ ,$$

where $G(E)$ is the pion-nucleus green function, $V(E)$ stands for a potential matrix, and P is projection operator, which projects onto the group of nuclear states being taken explicitly into account. The potential matrix

$$V(E)=V^{(1)}(E)+V^{(2)}(E)$$

receives the contribution from the first-order term $V^{(1)}(E)$, which can be expressed in terms of the elementary πN amplitude and nuclear form factors. The separable potential model was used to define the off-energy-shell extrapolation of πN amplitudes.

The phenomenological term $V^{(2)}(E)$ accounts for pion absorption and higher-order processes. This term was assumed to be diagonal in nuclear states and to be a scalar-isoscalar quantity. The functional form of its matrix element was chosen as the Fourier transform of the nuclear density squared and the energy dependence of the second-order potential was obtained by fitting the π-^{12}C scattering data. For further details we refer to Ref. 32.

A hybrid form of nuclear structure input was used in our calculations. The parameters of the symmetrized Fermi density of ^{15}N were obtained by fitting the longitudinal e-^{15}N form factor to experimental data. In doing this the proton and neutron density of ^{15}N were assumed to be the same. In the case of π-^{15}N elastic scattering, the ^{15}N spin form factors were calculated assuming the nucleus to be a pure $1p_{1/2}$ hole in the closed p shell of ^{16}O. The form factors were normalized by fitting the magnetic ^{15}N form factor to experimental data in the peak region.

As can be seen in Fig. 6, the calculations reproduce the cross section very well, which is a necessary condition for a reasonable prediction of a polarization observable. The analyzing power, however, is not reproduced. Unlike the large values of A_y predicted to occur near the minima in the differential cross section, the measured values are consistent with zero over the angular range 40° to 100° c.m. This did not change when the data were analyzed with the 9° angular acceptance of the SUSI spectrometer divided into two parts, thus verifying that there were no rapid angular variations of A_y which could have been averaged.

A large sensitivity of iT_{11} to the nuclear structure input was demonstrated in the case of π-^{6}Li elastic scattering.[19] At present it is not clear whether the serious discrepancies between theory and experiment for ^{15}N are due to incomplete knowledge of the nuclear structure or to some aspects of the scattering mechanism which is either neglected or not properly treated in the present calculation.

Analogous to the structure of ^{16}O, which is relatively well known, one could expect an admixture of higher configurations in the ground-state wave function of ^{15}N at the level of 20%. Therefore, our pure $p_{1/2}$-hole wave function may be inadequate for the calculation of reliable A_y values. Probably, an even more important source of ambiguities in the calculations presented here was the neglect of some Fermi motion terms. Due to the Fermi motion, the spin-flip part of the optical potential receives a contribution from the scalar part of the πN amplitude, which was not taken into account in our calculation. The effect of neglecting these terms in π-^{15}N elastic scattering was estimated and was found to be more than 50% for the analyzing power A_y^{22}. In view of the aforementioned ambiguities and other open questions discussed in detail in Ref. 22, we did not make any attempt to improve the agreement between the experimental and calculated A_y by fitting some parameters of the coupled-channels model.

Recently, Chakravarti has calculated the differential cross section and the analyzing power for π^+-^{15}N scattering at 164 MeV (Ref. 33) using the computer codes PIPIT (Ref. 34) and a modified version of ARPIN.[35] The spin-independent and spin-dependent pion nucleus amplitudes were obtained from the shell-model transition densities of Cohen and Kurath.[36] The distorted waves were calculated with a first-order optical potential using ground-state densities from electron scattering.

As one may expect from the similarity of the calculations the predictions of Chakravarti are almost identical to the ones from Mach up to 90° scattering angle. There are differences between the two calculations at larger angles, which is not surprising in view of the sensitivity of A_y in this angular region to details of the scattering mod-

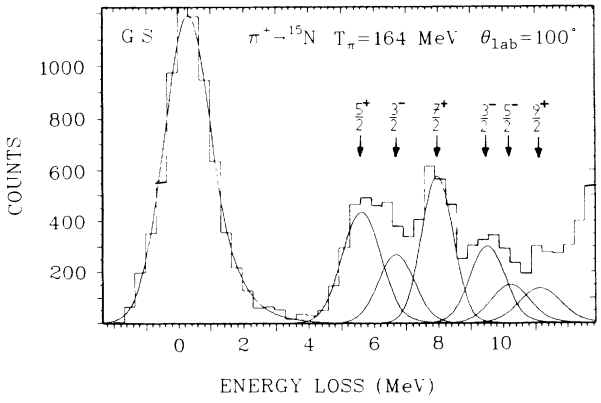

FIG. 7. Typical spectrum for elastic and inelastic pion scattering from polarized ^{15}N at $\theta_{lab}=100°$. The curves represent the peaks obtained with a multiple peak fitting program.

TABLE II. Results for A_y from the present experiment ($T_\pi = 164$ MeV) for ^{15}N excited states.

θ_{lab} (deg)	$\theta_{c.m.}$ (deg)	State	A_y	ΔA_y
90	91.2	$\frac{5}{2}^+$	−0.120	±0.242
		$\frac{3}{2}^-$	+0.132	±0.772
		$\frac{7}{2}^+$	+0.112	±0.262
100	101.2	$\frac{5}{2}^+$	−0.276	±0.347
		$\frac{3}{2}^-$	+0.591	±1.082
		$\frac{7}{2}^+$	+0.338	±0.343

els and wave functions.

Chakravarti also applied different quenching factors to the isoscalar spin dependent amplitudes and found that the near-zero asymmetry for the π^+-^{15}N data could only be reproduced by an unusually large quenching in comparison to commonly accepted quenching factors.[37]

Unfortunately, at present there are no Δ-hole calculations for π-^{15}N scattering, but they may become available in the future since the Δ-hole calculations which were originally only confined to closed-shell nuclei have now been extended to open-shell nuclei, not only for elastic and inelastic scattering[38] but also for charge exchange reactions.[39]

One should also keep in mind that at this pion energy the cross section displays a very diffractive structure. A large analyzing power is predicted only at the location of the deep minima of the cross section, the exact description of which is the most difficult part of the theory. For this reason future experiments should also investigate A_y below and above the (3,3) resonance where the cross sections are much less diffractive. Such measurements on ^{15}N—which are planned—together with systematic studies of spin effects for the neighboring nuclei ^{14}N and ^{13}C may shed some light on the present puzzle.

Important information may also be obtained from inelastic scattering from polarized nuclei. Due to the particular target configuration in this experiment, in most cases excited states in ^{15}N were not sufficiently well separated and the measured cross sections had low statistical accuracy. Therefore, in the present experiment, data could only be extracted with reasonable error bars at $\theta_{lab} = 90°$ and $\theta_{lab} = 100°$ for the $\frac{5}{2}^+$ and $\frac{7}{2}^+$ states. A typical spectrum for 100° is shown in Fig. 7. The curves represent the peaks obtained with a multiple peak fitting routine. The extracted analyzing powers are listed in Table II and displayed in Fig. 8. The errors contain the statistical uncertainty of foreground and background plus the uncertainty in the peak fitting.

In Fig. 8 we show the differential cross sections for the $(\frac{5}{2}^+, \frac{1}{2})$, $(\frac{3}{2}^-, \frac{1}{2})$, and $(\frac{7}{2}^+, \frac{1}{2})$ states at 5.27, 6.23, and 7.57 MeV, respectively,[40] the analyzing powers for two of those states and the theoretical predictions from Mach. In these calculations, the $(\frac{3}{2}^-, \frac{1}{2})$ state was assumed to be a pure $1p_{3/2}$ hole in the ^{16}O core. For the other two states, the transition form factors were calculated using the Millener-Kurath[41] wave functions. The coupling of

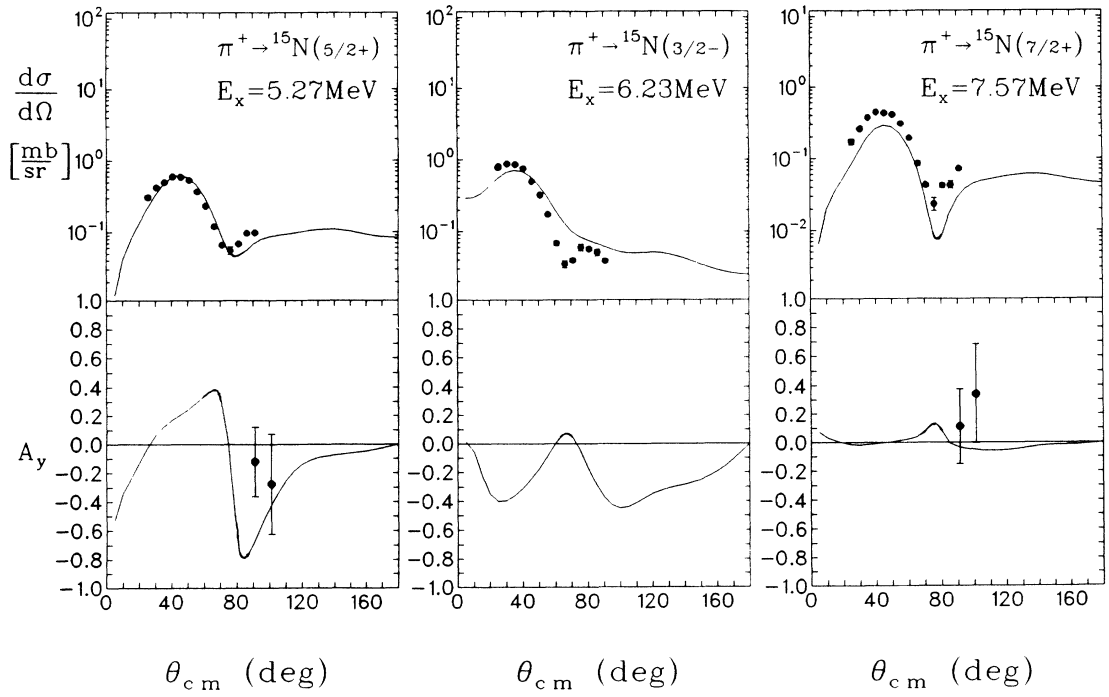

FIG. 8. Differential cross sections and analyzing powers for inelastic pion scattering from the $\frac{5}{2}^+$ (5.27 MeV), $\frac{3}{2}^-$(6.23 MeV), and $\frac{7}{2}^+$(7.57 MeV) states in ^{15}N. The cross-section data are from Ref. 40, the data for A_y from the present experiment and the curves are predictions from Mach.

each excited state to the ground state was assumed in our calculations.

Except for the $(\frac{7}{2}^+, \frac{1}{2})$ state the magnitude and shape of the cross sections is well reproduced. Within the limited accuracy of the measured analyzing power there is agreement with the theory. More precise data will be required for a more detailed comparison with the theory.

ACKNOWLEDGMENTS

This work would have been impossible without the generous help and considerable skills of the staff of the Paul Scherrer Institute. It was supported by the Bundesministeruim für Forschung and Technologie of the Federal Republic of Germany.

*Present address: Department of Physics, University of Regina, Regina, Saskatchewan, Canada S4S 0A2.

[1]E. T. Boschitz, in *Proceedings of the 7th International Conference on High Energy Physics and Nuclear Structure, Zürich 1977,* edited by M. Locher (Birkhäuser, Basel, 1978); C. H. Q. Ingram, in *Meson-Nuclear Physics—1979,* Proceedings of the 2nd International Topical Conference on Meson-Nuclear Physics, AIP Conf. Proc. No. 54, edited by E. V. Hungerford III (AIP, New York, 1979), p. 455. Nucl. Phys. **A374**, 319 (1982); D. Dehnhard, *ibid.* **A374**, 377c (1982); R. Redwine, *ibid.* **A434**, 239c (1985).

[2]L. S. Kisslinger, Phys. Rev. **98**, 761 (1955).

[3]R. Landau, S. Phatak, and F. Tabakin, Ann. Phys. (N.Y.) **78**, 299 (1973).

[4]L. C. Liu and C. M. Shakin, Phys. Rev. C **19**, 129 (1979).

[5]M. B. Johnson and D. J. Ernst, Phys. Rev. C **27**, 709 (1983).

[6]M. Gmitro, J. Kvasil, and R. Mach, Phys. Rev. C **31**, 1349 (1985).

[7]L. S. Kisslinger and W. L. Wang, Ann. Phys. (N.Y.) **99**, 374 (1976).

[8]E. Oset and W. Weise, Nucl. Phys. **A329**, 365 (1979).

[9]M. Hirata, F. Lenz and K. Yazaki, Ann. Phys. (N.Y.) **108**, 116 (1977).

[10]M. Hirata, J. H. Koch, F. Lenz, and E. J. Moniz, Ann. Phys. (N.Y.) **120**, 205 (1979).

[11]F. Vogler, R. Olszewski, M. Meyer, E. L. Mathie, G. Smith, E. Boschitz, S. Chakravarti, D. Dehnhard, and M. Thies, Phys. Lett. **134B**, 161 (1984); R. Olszewski *et al.*, Phys. Rev. Lett. **57**, 2143 (1986); Phys. Rev. C **37**, 2665 (1988).

[12]Proceedings of the LAMPF Workshop on Physics with Polarized Nuclear Targets, Los Alamos, New Mexico, 1986, edited by G. Burleson, W. Gibbs, G. Hoffmann, J. J. Jarme, and N. Tanaka (LANL Report No. LA-10772-C, 1986).

[13]R. Mach, Nucl. Phys. **A258**, 513 (1976).

[14]R. H. Landau, Phys. Rev. C **15**, 2127 (1977).

[15]D. Ernst, in Proceedings of the LAMPF Workshop on Physics with Polarized Nuclear Targets, Los Alamos, New Mexico, 1986, Ref. 12, p. 129.

[16]F. M. M. van Geffen, B. L. G. Bakker, H. J. Boersma, and R. van Wageningen, Nucl. Phys. **A468**, 683 (1987).

[17]J. A. Niskanen, L. Swift, and A. W. Thomas, Phys. Rev. C **40**, 2420 (1989).

[18]J. F. Germond, J. Phys. G **12**, 609 (1986).

[19]R. A. Eramzhyan, M. Gmitro, T. D. Kaipov, S. S. Kamalov, and R. Mach, J. Phys. G **14**, 1511 (1988).

[20]R. Nagaoka and K. Ohta, Ann. Phys. (N.Y.) **184**, 148 (1988).

[21]S. Chakravarti, LAMPF Research Proposal No. 1025 (unpublished).

[22]R. Mach and S. S. Kamalov, Nucl. Phys. **A511**, 601 (1990).

[23]R. Tacik *et al.*, Phys. Rev. Lett. **63**, 1784 (1989).

[24]R. Balsiger *et al.*, Nucl. Instrum. Methods **157**, 247 (1978); J. P. Albanese *et al.*, *ibid.* **158**, 363 (1979).

[25]G. R. Smith *et al.*, Phys. Rev. C **29**, 2206 (1984); **30**, 980 (1984).

[26]C. R. Ottermann *et al.*, Phys. Rev. C **38**, 2296 (1988); **38**, 2310 (1988).

[27]G. R. Court, W. G. Heyes, W. Meyer, and W. Thiel, in *Proceedings of the Fourth International Workshop on Polarized Target Materials and Techniques, Bad Honnef, West Germany, 1984,* edited by W. Meyer (University of Bonn, Bonn, West Germany, 1984), p. 53; R. Dostert *et al.*, *ibid.*

[28]R. A. Arndt and L. O. Roper, SAID Phase Shift Analysis Program, Virginia Politechnical Institute and State University.

[29]S. J. Seestrom-Morris *et al.*, Phys. Rev. C **31**, 923 (1985).

[30]F. Binon *et al.*, Nucl. Phys. **A298**, 499 (1978).

[31]M. E. Sevior *et al.*, Phys. Rev. C **40**, 2780 (1989).

[32]M. Gmitro, S. S. Kamalov, and R. Mach., Phys. Rev. C **36**, 1105 (1987).

[33]S. Chakravarti, University of Minnesota report, 1990.

[34]R. A. Eisenstein and F. Tabakin, Comput. Phys. Commun. **12**, 237 (1976).

[35]T.-S.H. Lee and D. Kurath, Phys. Rev. C **21**, 293 (1980).

[36]S. Cohen and D. Kurath, Nucl. Phys. **A226**, 253 (1974).

[37]I. S. Towner, Phys. Rep. **155**, 264 (1987).

[38]R. Nagaoka and K. Ohta, Ann. Phys. **184**, 148 (1988). K. Junker and E. Levin (unpublished).

[39]N. Ohtsuka, Nucl. Phys. **A480**, 513 (1988).

[40]D. Dehnhard (private communication).

[41]D. J. Millener and D. Kurath, Nucl. Phys. **A255**, 315 (1975); H. R. Kissener, H. V. Jäger, and O. Richter, JINR Dubna Report No. E4-90-57, 1990 (unpublished).